JOURNAL OF CATALYSIS 118, 339–348 (1989)

Oxygen Storage Capacity of Noble Metal Car Exhaust Catalysts Containing Nickel and Cerium

P. LÖÖF, B. KASEMO, AND K.-E. KECK

Physics Department, Chalmers University of Technology, S-41296 Göteborg, Sweden

Received April 6, 1988; revised February 9, 1989

Oxygen storage capacity as a function of temperature was measured for two different monolithic car exhaust catalysts. Mass spectrometry connected on-line to a flow reactor was used for quantification of oxygen uptake and reduction, respectively. Both catalysts contained Pt, Rh, and Ce supported by Al_2O_3. One of the catalysts also contained Ni. The amount of oxygen that can be taken up/reduced away is strongly temperature-dependent in the range investigated (300–900 K). When present, Ni dominates the oxygen storage capacity at high temperatures. In the catalyst lacking Ni, Ce dominates the storage capacity at high temperatures. At lower temperatures chemisorbed oxygen on Pt/Rh seems to play an essential role.

1. INTRODUCTION

The purpose of a car exhaust catalyst is to simultaneously reduce CO, C_nH_m, and NO_x emission from automotive exhaust (*1*). The requirement that both reduction of NO and oxidation of CO and C_nH_m must occur simultaneously demands precise control of the air/fuel ratio and sophisticated composition of the catalyst. To improve the performance of the catalyst and make it less sensitive to small temporary variations in the air/fuel ratio a so-called oxygen "storage" component is frequently added to the catalyst. This component is usually a metal (oxide) component which may be reversibly oxidized and reduced at typical operating temperatures of the catalyst. Among several metal oxide candidates (*2*) cerium and nickel (oxides) have been most commonly used for this purpose (*3–5*). Additional oxygen storage may be obtained via chemisorbed oxygen on the catalytically active noble metal particles of the catalyst.

Gandhi *et al.* (*2*) found a substantial oxygen storage capacity in four different commercial monolithic catalysts when prereduced by 2% CO in He at 500°C. Hertz (*3*) made a study of a Ce-containing three-way catalyst and found direct evidence that the oxygen content of the catalyst varied with engine exhaust composition. The measured amounts and rates of change of oxygen were found to be sufficiently large to affect the performance of the catalyst under dynamic operating conditions. Yao and Yu Yao (*4*) examined the oxygen storage capacities of CeO_2, CeO_2/Al_2O_3, and *PM*/CeO_2/Al_2O_3 and showed that they were significant and increased with increasing temperature in the order from CeO_2 to *PM*/CeO_2/Al_2O_3 (*PM* stands for "Precious Metal", i.e., Pt, Rh, etc.). Su *et al.* (*5*) investigated the dynamic oxygen storage capacity of three-way catalysts using CO and O_2 pulses at 500 and 600°C. When CeO_2 was added to the *PM* catalysts a significant increase in the oxygen storage capacity was observed. Addition of NiO also enhanced the oxygen storage capacity but only under mild thermal pretreatment. Cooper and Keck (*6*) also observed that NiO plays a role in fresh catalyst systems but its effect disappeared upon aging, probably because highly dispersed nickel forms a surface nickel–aluminate complex, which minimizes oxygen storage capacity. They found that catalysts which contain stable NiO are

0021-9517/89 $3.00

capable of maintaining a higher storage capacity after aging at 980°C in 10% H_2O/N_2.

In this work we have studied the absolute oxygen storage capacity as a function of temperature for two commercial, monolithic, three-way car exhaust catalysts in a specially developed flow reactor. The absolute oxygen storage capacity was measured by consecutive cycles of reduction (in CO and H_2, respectively) and oxidation in O_2.

Quantitative results are presented for the oxygen uptake as a function of temperature, after reduction in H_2 and CO, respectively.

2. EXPERIMENTAL

The experimental system is shown schematically in Fig. 1. This system is a modification of a system described earlier (*7*). Four different gases can be injected into the reaction cell (C, D) via four manually operated valves (A). The different gases enter the cell in a mixing volume (B). The reaction cell consists of two quartz tubes (C, D). The inner tube (D) (outer diameter 12 mm, inner diameter 10 mm, and length 200 mm) has a constriction in one end, where the catalyst (F) is mounted. The inner tube is enclosed in an outer tube (C) with a length of 250 mm and an outer diameter of 15 mm. The reaction cell is connected to the inlet and outlet systems by vacuum-tight Viton O-rings. Heating of the gas flow is achieved by an external heating coil (G). In order to improve heat transfer and mixing of the gases, the inner tube is filled with quartz rods and quartz wool. The gas flow is measured and controlled by Porter flow meters. The cell can be used for gas flows up to 10 liter/min. With valves (H) and (A) closed, the cell can be evacuated by roughing or diffusion pumps of the vacuum system connected via the valve (H). The temperature is measured by a chromel–alumel thermocouple (diameter 0.1 mm) located in one of the channels of the monolithic catalyst sample.

A minute amount of the gas flow is sampled through a quartz tube orifice leak (*7, 8*) at (I) mounted in the holder (K) and fed into the vacuum system where it is continuously analyzed by a quadrupole mass spectrometer (O, P, Q). The temperature and mass spectrometer signals are registered by a strip chart recorder. A complementary way to measure the change in gas temperature is to record the change in the

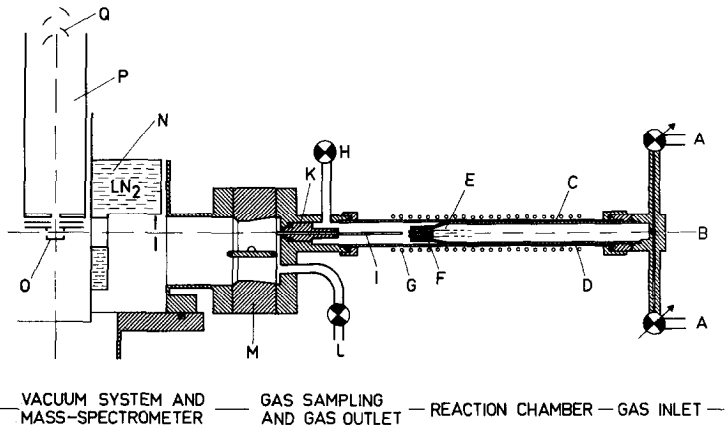

FIG. 1. The gas mixture is introduced at A, is preheated by the heating coil (D), and flows through the monolithic catalyst F. A quartz tube (I) with a small orifice at its tip, samples gas at the catalyst outlet side (*7, 8*). The tip is positioned close to the catalyst to optimize the response time. At the gas flows used in this work the overall response time is determined by the gas flow time from A to F (approximately 2 s).

intensity of the Ar signal when the temperature is changed (*7*). The tip of the quartz leak is positioned on the central axis of the reaction cell, about 4 mm from the catalyst sample. The system response time for measurements of variations in the partial pressures at the tip of the quartz leak is about 50 ms under 1 atm total pressure (*7*). The time required for the gas to reach the catalyst from the injection valves was measured to be about 2.0 s at a gas flow of 200 ml/min (see curve (a) in Fig. 2).

The catalysts investigated in this work were cut out from two different, fresh, monolithic, three-way car exhaust cleaners from Engelhard Industries. The noble metal content (except for rhodium) and the base metal content in the catalyst were analyzed by X-ray fluorescence. The results are presented in Table 1. According to the manufacturers specification the rhodium content is one-fifth of the platinum content. The support is cordierite with a wash-coat of γ-alumina. As can be seen in Table 1 the

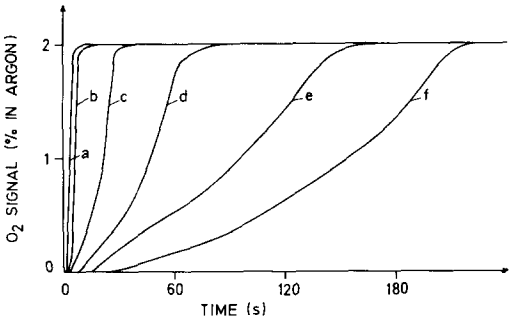

FIG. 2. Oxygen concentration vs time at the outlet of a monolithic car exhaust catalyst (catalyst A), exposed to a flow of 2% O_2 in Ar. The O_2/Ar mixture was introduced at $t = 0$. Prior to the O_2 exposure the catalyst has been reduced in CO at 900 K. The curve labeled (a) is obtained with an oxygen-saturated catalyst and gives the system response. Curves (b)–(f) were obtained at catalyst temperatures of 370, 460, 600, 730, and 900 K, respectively. From the area between a particular curve ((b)–(f)) and curve (a) the absolute oxygen-uptake amount at that temperature can be determined. These results are summarized in Fig. 3 as oxygen uptake vs temperature.

TABLE 1

Composition of the Catalysts

Element	Catalyst A		Catalyst B	
	wt%[a]	Rel. atom.%[b]	wt%[a]	Rel. atom.%[b]
Ce	0.8	7.3	1.0	34.0
Cr	0.05	1.22	0.08	7.5
Fe	0.5	11.35	0.3	26.0
Ni	3.1	67.35	0.01	0.8
La	0.03	0.28	0.03	1.0
Pt	0.16	1.04	0.16	4.0
Sm	0.15	1.27	0.15	4.8
Ti	0.37	9.8	0.2	20.5
Rh	0.03	0.37	0.03	1.4
Total	5.19	100	1.96	100

Note. The left column for each catalyst gives the weight percentages of the various constituents. 100% corresponds to the total catalyst weight (monolithic support + washcoat + base metals + noble metals). The right columns are the relative atomic concentrations of the elements listed in the table (base metals + noble metals). The concentrations were determined by X-ray-induced X-ray fluorescence.

[a] In percent of the total catalyst weight.

[b] Relative atomic concentrations of the elements listed in the table.

two catalysts labeled A and B have similar analyses except in nickel content where there is a marked difference (3.1 and 0.01 wt%, respectively). The weight, length, and diameter of the samples were 1.26 g, 20 mm, and 8 mm, respectively. Each sample consisted of about 30 longitudinal channels.

The gases used were of ultrahigh purity (99.9997% purity) and the gas flow was 200 ml/min, which corresponds to a space velocity of 12000 hr^{-1}. The samples were oxidized by a gas flow of 2% O_2 in Ar and the catalysts were reduced in a flow of 4% CO in Ar or 4% H_2 in Ar.

The relative sensitivity for different gases of the mass spectrometer was determined by use of known mixtures of CO, O_2, etc., in Ar. Control runs with the reaction cell empty (i.e., no catalyst) were performed at regular intervals to check that wall reactions did not take place.

3. RESULTS

3.1. Oxygen Uptake as a Function of Temperature after Reduction in CO at 900 K

In the first series of experiments the Ni-containing catalyst (A) was first reduced in CO at 900 K. The oxygen uptake was then measured at different constant temperatures. The exact experimental sequence was the following: The catalyst was first oxidized in a gas flow of 2% O_2 in Ar under 1 atm and 900 K for 10 min, to remove possible carbon contamination. The gas flow was then changed to a mixture of 4% CO in Ar, which was allowed to flow for 10 min at 900 K. During this treatment the surface was reduced, which could be observed via the CO_2 mass spectrometer signal. The choice of 900 K as the reduction temperature was a compromise to avoid CO disproportionation occurring at lower temperatures (*9*) and the structural changes occurring at considerably higher temperatures.

When the reduction sequence was completed, the gas flow was changed to pure Ar and the temperature of the reaction cell and catalyst was lowered over a period of 7 min to the temperature at which the oxygen uptake measurement was to be made. The gas flow was then changed from Ar to 2% O_2 in Ar. The O_2 concentration at the outlet side of the catalyst was continuously monitored by the mass spectrometer. Figure 2 shows a set of such curves of O_2 signal vs time for catalyst A for five different temperatures, (b) 370 K, (c) 460 K, (d) 600 K, (e) 730 K, and (f) 900 K, respectively. Curve (a), which is a reference curve showing the system response, was recorded with an oxygen-saturated catalyst.

The time delay in the rise of the O_2 signal in curves (b)–(f) as compared with curve (a) is caused by the uptake of oxygen by the catalyst. The difference $\int_0^\infty (I^a_{O_2}(t) - I^i_{O_2}(t))dt$ ($i = b, c, d, e, f,$) between the reference curve (a) and a specific curve (i), is proportional to the amount of oxygen uptake (I_{O_2} = mass spectrometer signal for O_2). The uptake can be quantified by use of the known concentration of O_2 in the inlet gas and the known flow velocity.

Figure 3a shows a plot of the oxygen uptake determined in this way (crosses and dashed curve) as a function of the uptake temperature. The left-hand vertical axis gives the uptake in micromoles of oxygen per gram of catalyst and the right-hand axis gives the estimated O/Ni ratio obtained if all oxygen is assumed to be bound to Ni. Guided by the corresponding results with H_2 as the reducing gas and by the observation that the estimated O/Ni ratio is close to one, we expect that the oxygen uptake at 900 K is close to saturation.

When an oxygen uptake run had reached saturation the catalyst was again heated in O_2 at 900 K and thereafter reduced in CO as described above. A new uptake run could then be performed. The reduction in CO after oxygen uptake could be followed via the CO_2 evolution and the delay in the rise of the CO signal (see Fig. 4). The integrated amount of CO_2 and the integrated delay in the CO signal gave independent measures

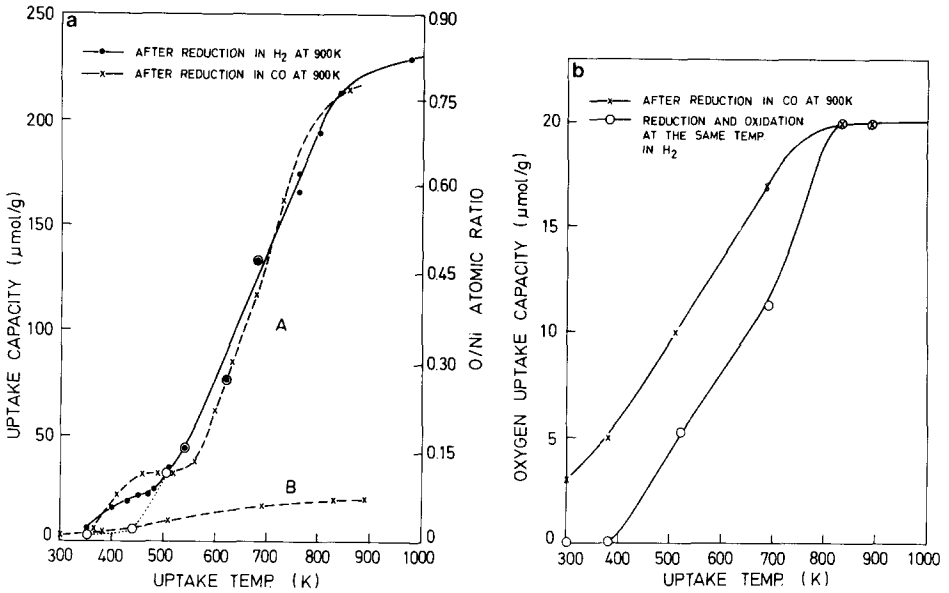

FIG. 3. (a) Oxygen uptake capacity as a function of uptake temperature for two different (A and B) monolithic car exhaust catalysts. Catalyst A contains Ni and Ce, catalyst B contains no Ni. The curves labeled (x) and (●) were obtained by reducing in CO and H_2, respectively, at 900 K and the oxygen uptake was then measured at the temperature given on the abscissa. The curve labeled (○) was measured by performing both the reduction in H_2 and the uptake measurement at the same temperature. (b) Oxygen uptake vs uptake temperature for catalyst B, without Ni. The oxygen uptake was measured at each temperature after reduction in CO at 900 K (x) or after reduction in H_2 at the same temperature as the uptake temperature (○).

of the oxygen uptake. The three types of uptake determination agreed within the experimental errors (≤5% of the uptake); i.e., mass balance was obtained in the measured results.

The oxygen uptake by catalyst B (without Ni) was also investigated using CO as the reducing gas. The result is displayed at the bottom of Fig. 3a and in Fig. 3b. The uptake by this catalyst is more than an order of magnitude smaller than that by catalyst A, demonstrating the importance of Ni for the oxygen uptake of the fresh catalyst.

3.2. *Influence of CO Disproportionation during Reduction*

A word of caution is necessary concerning reduction in CO. If it is performed considerably below 900 K, CO disproportionates on nickel via the reaction $CO + CO \rightarrow CO_2 + C$ and carbon is deposited on the catalyst. (The conclusion that Ni is responsible for the disproportionation was drawn from the observation that little or no disproportionation occurred on the catalyst without Ni.) The maximum disproportionation rate occurs around 700 K, and large amounts of carbon can be deposited (*9*). During a subsequent oxygen uptake run of the type shown in Fig. 2, oxygen is then consumed both due to oxidation of base metals and due to oxidation of carbon of CO_2. If one is not aware of this, large errors in the determination of the oxygen uptake capacity may result, both with volumetric and manometric methods. The best way to eliminate effects of this side reaction is to look for CO_2 production by the MS during the oxygen uptake measurement or alternatively to use H_2 as the reducing gas. The absence of CO_2 produc-

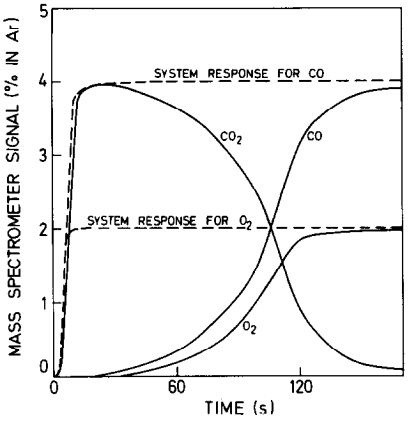

FIG. 4. Mass spectrometer signals vs time at the catalyst outlet for CO and CO_2 during reduction, and for O_2 during uptake (oxidation) measurements, respectively, at 900 K. The dashed curves are the system responses for CO and O_2, respectively, in the absence of reaction. The CO and CO_2 signals were recorded simultaneously when 4% CO in Ar was flowed over the oxidized catalyst. The O_2 signal was recorded when 2% O_2 in Ar was flowed over the reduced catalyst. Flow 200 ml/min. The gas mixtures were introduced at $t = 0$. Oxidation and reduction runs were performed on the same sample. (Note that mass balance is approximately obtained in that the area under the CO_2 curve is equal to the area between the dashed line and the full curve for CO, and also equal to twice the area between the dashed line and the full curve for O_2.)

tion during oxygen uptake and mass balance between oxygen uptake after reduction, and CO_2 production during reduction, showed that CO disproportionation was avoided in this work.

3.3. Oxygen Uptake after Reduction in H_2

Exactly the same experimental series as described in Section 3.1 was performed for catalyst A with H_2 replacing CO as the reducing gas. The resulting oxygen uptake vs uptake temperature curve is shown in Fig. 3a (solid circles, full curve). The experimental point measured at 950 K indicates saturation in the uptake around this temperature. Above 600 K the results obtained with CO and H_2 coincide within the experimental uncertainties. A slight but significant difference is seen in the temperature range 430–570 K where the catalyst reduced in CO shows a distinct plateau in the oxygen uptake. The plateau is replaced by a change in slope in the results obtained with H_2.

A series of experiments was also performed where both reduction and oxidation were performed at the same temperature. (This was not meaningful with CO due to the CO disproportionation discussed above.) The oxygen uptake for catalyst A vs oxidation/reduction temperature from this experiment is shown by the open circles and dotted curve in Fig. 3a. At temperatures above 500 K these results coincide with the ones where reduction was performed at 900 K, but below 500 K incomplete reduction obviously reduces the oxygen uptake in comparison with the result obtained after reduction at 900 K. For catalyst B, without Ni, the results from this type of experiment coincide only at temperatures >830 K but differ considerably at lower temperatures, again indicating that incomplete reduction lowers the oxygen uptake below 830 K. Results from oxidation and reduction at the same temperature for catalyst B are shown by the open circles in Fig. 3b.

4. DISCUSSION

4.1. Amounts of Oxygen Uptake and Distribution of Oxygen among Oxygen-Carrying Elements

The possible oxygen-carrying elements that we need to consider are given in Table 1 with their weight percentages relative to the total catalyst weight and also with their relative atomic percentages. We restrict the discussion to Ni, Ce, Pt, and Rh for the following reasons: Ni is obviously the main oxygen carrier in catalyst A, as can be seen by comparing the uptakes of catalysts A and B. Ce dominates in quantity over La and Sm, and has previously been identified as an important oxygen "storage" element. Concerning Fe and Ti it is obvious from comparisons of the results from catalyst A and B that they can be neglected in catalyst A. Furthermore it is most likely that Fe and

Cr are contained in the monolith. In the case of catalyst B we cannot exclude that Fe and/or Ti contributed to the oxygen storage. Pt and Rh are considered despite their small amounts because of their high dispersion and because they both may carry significant amounts of chemisorbed oxygen available for oxidation reactions, and Rh may also carry oxygen as a bulk oxide.

Table 2 gives the concentrations of Ni, Ce, Pt, and Rh and their respective maximum oxygen storage capacity (in μmol/g), and also relative concentrations of surface atoms assuming (somewhat arbitrarily) 50% dispersion for Pt and Rh and 10% dispersion for Ni and Ce. The dispersion assumptions are made only for the sake of discussion. However, recent STEM pictures of noble metal particles on catalysts from the same manufacturer as catalysts A and B in this work, indicate a dispersion $\geq$30% (*12*). Since the smallest particles are probably not detected, the dispersion is probably somewhat larger. (Aged catalysts have much smaller dispersions.) The assumed dispersion for Ni is more arbitrary, but is used only for discussion purposes. For comparison a dispersion of 1% is also considered. The maximum experimental uptakes of oxygen, obtained from the curves in Fig. 3, are given at the bottom of each table. The maximum uptake of catalyst A, 240 μmol/g, is very close to the maximum oxygen storage capacity of Ni in that catalyst, assuming complete oxidation/reduction. It corresponds to about 80% of the total oxygen capacity of Ni, Ce, Pt, and Rh together, assuming complete oxidation of all elements to NiO, CeO_2 (from Ce_2O_3), PtO_2, and RhO_2. (These numbers are given only for comparative purposes. We do not expect that Pt oxidizes to PtO_2.)

The maximum uptake of catalyst B, 20 μmol/g, is very close to the total capacity of Ce for this catalyst and corresponds to about 60% of the summed capacity of Ce, Pt, and Rh and to about 80% of the capacity if bulk oxidation of Pt is excluded. We conclude that Ni is almost completely re-

TABLE 2

Oxygen Storage Elements

Component	Concentration (wt%)[a]	Relative conc. of surface atoms (%)	Max. oxygen storage capacity (μmol/g)	Max. exptl. oxygen uptake (μmol/g)
Catalyst A				
Ni	3.1	82.4	270.6	
Ce	0.8	8.9	15.7	
Pt	0.16	6.4	9.2	
Rh	0.03	2.3	3.2	
Total	4.09	100	298.7	240
Catalyst B				
Ni	0.01	1.3	0.9	
Ce	1.0	55.5	19.6	
Pt	0.16	32.0	9.2	
Rh	0.03	11.5	3.2	
Total	1.20	100	32.9	20

Note. The left column gives the weight percentages (of total catalyst weight) of oxygen storage candidates for catalyst A and B, respectively. The right column gives the maximum oxygen storage capacity, and the middle column the relative atomic concentrations of surface atoms of the oxygen storage elements, assuming 10% dispersion for Ni and Ce and 50% dispersion for Rh and Pt. Note the dominance of Ni in catalyst A and that Pt and Rh together have approximately half the capacity of Ce in catalyst B.

[a] In percentage of total catalyst weight.

duced and oxidized, respectively, at 900 K and above, and is the main oxygen carrier at high temperatures in catalyst A. For catalyst B the interpretation is less unambiguous. The measured oxygen capacity is larger than that obtained if we consider complete oxidation of Pt and Rh alone. We would not, however, expect complete oxidation of Pt in the present conditions, and neither do we expect the nearly 100% dispersion which would be necessary to associate the major part of the oxygen uptake of catalyst B with Rh and Pt alone. If we in contrast consider Ce alone, we find that the measured uptake is almost exactly corresponding to the reaction $Ce_2O_3 \rightleftarrows CeO_2$. Complete reduction of CeO_2 is, however, not expected at 900 K but only at temperatures $\geq$1075 K (*4*). The likely degree of reduction of Ce is $CeO_2 \rightleftarrows CeO_{2-x}$ with $x \leq 0.3$ (*4*). We can thus only account for about 60% of the measured oxygen capacity of catalyst B by attributing it to Ce alone. The most likely complementary candidate is Rh which by complete oxidation/reduction according to $Rh \rightleftarrows RhO_2$ could account for about 15% of the capacity. Of the residual $\approx$25% some fraction could be attributed to oxygen chemisorption on Pt which could account for at most $\approx$5% at 50% dispersion (1/2 ratio between surface atoms of O and Pt). It thus seems likely that one or more of the elements Fe, Cr, and Ti (see Table 1) also participates. For example, if we assume that titanium undergoes the same oxidation reduction cycles as Ce, $TiO_2 \rightleftarrows TiO_{2-x}$, $x \leq 0.3$, it can account for about 10% of the capacity. In summary, for catalyst B, its maximum oxygen capacity seems to be dominated by cerium oxide, with significant contributions also from Rh, Pt (chemisorption) and Ti, and/or Fe and Cr.

In the temperature range below 900 K and down to about 500 K the oxygen storage capacity decreases rapidly. For the Ni-containing catalyst this is attributed to successively less and less complete oxidation of Ni with decreasing temperature. Below 500 K the oxygen uptake by chemisorption on all elements may be significant. Assuming that one oxygen atom can be chemisorbed at saturation per two surface metal atoms (typical for Ni and Pt), and the same assumed dispersions as above, we obtain a maximum chemisorption capacity on catalyst A of 9 μmol/g, i.e., equal to the total uptake around 350 K. In this temperature range and below, chemisorbed oxygen may thus play an important role.

On catalyst B chemisorbed oxygen on Pt and Rh is likely to play a relatively larger role in the uptake since their maximum chemisorption capacity corresponds to $\approx$7% of thee total oxygen capacity of this catalyst.

4.2. Mechanistic Considerations

The oxidation/reduction reactions that we consider are the following:

(i) $Ni + \frac{1}{2}O_2 \rightleftarrows NiO$

(ii) $CeO_{2-x} + \frac{1}{2}x\ O_2 \rightleftarrows CeO_2$

(iii) $Pt\text{-surface} + O_2 \rightleftarrows Pt + \text{chemisorbed O}$

$Pt + O_2 \rightleftarrows PtO_2$

(iv) $Rh + O_2 \rightleftarrows RhO_2$

Dissociative oxygen chemisorption on Rh may also be important. We are neglecting alloying or inmixing of the actual metallic components in the alumina wash coat, which may complicate the oxidation/reduction behavior. Oxidation of Pt and Rh would not be expected based on their behavior as bulk metals in a pure form. However, both the high dispersion of the noble metals and the presence of impurities may change the situation (*10, 11*). The roles of Pt and Rh as oxygen carriers are expected to be important particularly at the lowest temperatures where chemisorbed oxygen is much more available for oxidation of CO or hydrocarbons than oxygen in CeO_2 or NiO. (Pt and Rh are excellent oxidation catalysts far below the temperatures where NiO becomes nonreducible.)

At higher temperatures >500 K we attribute the increasing oxygen uptake of catalyst A to an increasing oxide thickness on the surfaces of the Ni particles, until they are

completely oxidized around 900–1000 K. If we assume 10% dispersion of Ni and a cubic particle shape we arrive at a maximum oxidation depth at saturation of 45 Å. If we instead assume 1% dispersion this figure becomes 450 Å. If a half-spherical particle shape is assumed the corresponding numbers are 33 and 330 Å, respectively.

For catalyst B we attribute the increasing uptake with temperature to increasing oxidation depth of CeO_{2-x}, $x \approx 0.3$, toward CeO_2 but with contributions also from oxidation of Rh to RhO_2 and from oxidation of partly reduced Ti, Fe, and/or Cr oxides. A significant difference between catalysts A and B is that lowering of the reduction temperature influences the oxygen uptake only below 500 K for catalyst A, but already around 800 K for catalyst B (open circles in Figs. 3a and 3b). This indicates that Ni is more easily reduced than CeO_2 in these catalysts.

4.3. Implications of the Present Results for Practical Systems

The relatively strong temperature dependences of the oxygen uptake and of the reduction reaction show that the amount of oxygen available for CO and hydrocarbon oxidation, respectively, is much smaller at lower temperatures. For example, the maximum available oxygen amount in catalyst A under dynamic conditions at 400 K is sufficient for oxidation of CO and C_mH_n over 3 s under typical engine conditions, while the corresponding time at 900 K is 20 s. (This estimate was made assuming the following: (a) catalyst weight of 700 g (b) engine with a cylinder volume of 2 liters, (c) 1% CO in the exhaust and 0.1% C_mH_n, and (d) engine revolution of 3000 rpm.) The observation that a lowering of the reduction temperature below 900 K influences the dynamic oxygen storage capacity of CeO_2 already at 900 K but that of NiO at 500 K would favor Ni as the storage element below 800 K. However, Cooper and Keck (*6*) found that the oxygen storage capacity of NiO disappeared upon aging, probably because of nickel–aluminate formation.

At temperatures below 500 K chemisorbed oxygen on Pt and Rh is expected to be important in the dynamic oxygen storage capacity. Their estimated maximum capacity (at 50% dispersion and O/Pt = 1/2) corresponds to oxidation of CO and C_nH_m over 0.05 s under typical conditions.

An interesting effect is the strong CO disproportionation around 700 K (*9*), which if it occurs under real conditions actually may help in reducing CO emissions under fuel-rich conditions and NO emissions under oxygen-rich conditions (since O_2 and also NO may be consumed by oxidation of the deposited carbon).

The composition of engine exhausts entering a "three-way" catalyst oscillates around the stoichiometric point at frequencies of 0.5 to 2 Hz when the engine is operating under feedback control (*3*). Therefore it is not only the total amount of oxygen that can be stored and then reduced away which is important in the dynamic performance of the catalyst (*3*). The reduction and oxidation rates are also important. Curves (d), (e), and (f), in Fig. 2 show that the initial oxidation rate in O_2 is fast enough to completely consume all O_2 in the gas stream. The time required to achieve complete oxidation of the catalyst is not determined then by the oxidation rate but by the mass transport of O_2 to the catalyst. When the oxidized catalyst is exposed to CO, the shape of the CO signal curve is approximately that of the O_2 signals (see Fig. 4). The initial reduction rate is thus fast enough to remove all CO in the gas stream.

In summary this study shows that both oxygen storage capacity and the oxidation and reduction rates are large enough to improve the performance of the two investigated catalysts under dynamic operating conditions.

SUMMARY

We have performed quantitative measurements of oxygen storage capacity on catalysts containing Pt, Rh, Ni, and Ce supported on Al_2O_3. At high temperatures Ni is the dominant storage metal and Ce

dominates over Pt and Rh. At low temperatures chemisorption on Pt and Rh may be important. The time constant for uptake/removal of oxygen on all these metals is sufficiently small at higher temperatures to make it important in practical systems, while at lower temperatures chemisorbed oxygen may be dominant.

ACKNOWLEDGMENTS

This project was financially supported by the National Swedish Board for Technical Development (Contract 83-5405). We are grateful to Mats Öblad, who performed the X-ray fluorescence analysis. We are also grateful for financial support from EKA Nobel AB during the later stage of this work.

REFERENCES

1. Wei, J., *in* "Advances in Catalysis" (D. D. Eley, P. W. Selwood, and Paul B. Weisz, Eds.), Vol. 24. Academic Press, New York, 1975.
2. Gandhi, H. S., Piken, A. G., and Shelef, M., Society of Automotive Engineers, Paper No. 760201 (1976).
3. Herz, R. K., *Ind. Eng. Chem. Prod. Res. Dev.* **20,** 451 (1981).
4. Yao, H. C., and Yu Yao, Y. F., *J. Catal.* **86,** 254 (1984).
5. Su, E. C., Montreuil, C. N., and Rothschild, W. G., *Appl. Catal.* **17,** 75 (1985).
6. Cooper, B. J., and Keck, L., Society of Automotive Engineers, Paper No. 800461 (1961).
7. Kasemo, B., Keck, K.-E., and Högberg, T., *J. Catal.* **66,** 441 (1980).
8. Kasemo, B., *Rev. Sci. Instrum.* **50,** 1602 (1979).
9. Lööf, P., and Kasemo, B., in press.
10. Hertz, R. K., and Shinouskis, E. J., *Appl. Surf. Sci.* **19,** 373 (1984).
11. Oh, S. H., and Carpenter, J. E., *J. Catal.* **80,** 472 (1983).
12. Stenbom, B., M.S. thesis, Chalmers University of Technology, Gothenburg, 1988.